analytical chemistry

Article

Cite This: Anal. Chem. XXXX, XXX, XXX−XXX

pubs.acs.org/ac

Peptide Disc Mediated Control of Membrane Protein Orientation in Supported Lipid Bilayers for Surface-Sensitive Investigations

Alessandra Luchini,*[,†] Frederik Grønbæk Tidemand,[†] Nicolai Tidemand Johansen,[†] Mario Campana,[‡] Javier Sotres,[§] Michael Ploug,[∥,⊥] Marité Cárdenas,[§] and Lise Arleth*[,†]

[†]Niels Bohr Institute, University of Copenhagen, Universitetsparken 5, 2100 Copenhagen, Denmark

[‡]ISIS-STFC, Rutherford Appleton Laboratory, Chilton, Oxon OX11 0QX, United Kingdom

[§]Biofilms Research Center for Biointerfaces and Department of Biomedical Science, Faculty of Health and Society, Malmö University, Per Albin Hanssons Väg 35, 214 32 Malmö, Sweden

[∥]Biotech Research and Innovation Center, University of Copenhagen, Ole Maaløes Vej 5, 2200 Copenhagen, Denmark

[⊥]Finsen Laboratory, Rigshospitalet, Ole Maaløes Vej 5, 2200 Copenhagen, Denmark

Supporting Information

ABSTRACT: In vitro characterization of membrane proteins requires experimental approaches providing mimics of the microenvironment that proteins encounter in native membranes. In this context, supported lipid bilayers provide a suitable platform to investigate membrane proteins by a broad range of surface-sensitive techniques such as neutron reflectometry (NR), quartz crystal microbalance with dissipation monitoring (QCM-D), surface plasmon resonance (SPR), atomic force microscopy (AFM), and fluorescence microscopy. Nevertheless, the successful incorporation of membrane proteins in lipid bilayers with sufficiently high concentration and controlled orientation relative to the bilayer remains challenging. We propose the unconventional use of peptide discs made by phospholipids and amphipathic 18A peptides to mediate the formation of supported phospholipid bilayers with two different types of membrane proteins, CorA and tissue factor (TF). The membrane proteins are reconstituted in peptide discs, deposited on a solid surface, and the peptide molecules are then removed with extensive buffer washes. This leaves a lipid bilayer with a relatively high density of membrane proteins on the support surface. As a very important feature, the strategy allows membrane proteins with one large extramembrane domain to be oriented in the bilayer, thus mimicking the in vivo situation. The method is highly versatile, and we show its general applicability by characterizing with the above-mentioned surface-sensitive techniques two different membrane proteins, which were efficiently loaded in the supported bilayers with ∼0.6% mol/mol (protein/lipid) concentration corresponding to 35% v/v for CorA and 8% v/v for TF. Altogether, the peptide disc mediated formation of supported lipid bilayers with membrane proteins represents an attractive strategy for producing samples for structural and functional investigations of membrane proteins and for preparation of suitable platforms for drug testing or biosensor development.

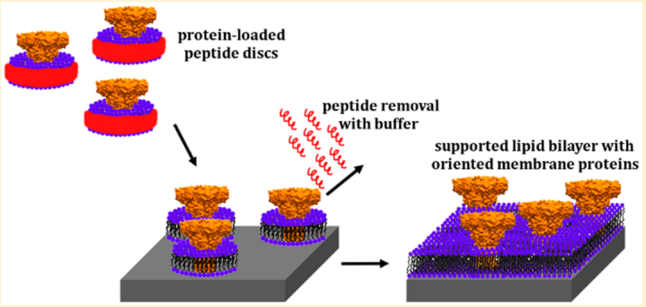

Membrane proteins are fundamental cell membrane components with vital biological functions. However, relatively little structural and functional information is available compared to soluble proteins. Indeed, membrane proteins are generally difficult to study with standard biophysical methods including X-ray crystallography. On top of this, it is well-known that the native structure of a membrane protein is strongly dependent on its surrounding lipid environment, which introduces further complexity in sample preparation and limits the choice of the experimental methods for probing the protein structure.[1]

In the cell, all copies of a given membrane protein have the same orientation of their extramembrane domains with respect to the biomembrane. Hence, controlling membrane protein orientation is particularly relevant to simulate their native arrangements in cell membranes.[2] Supported membranes composed of a lipid bilayer in the proximity of a solid support represent an attractive strategy for reproducing the native lipid environment of membrane proteins.[3−6] They enable the assembly of a plethora of different lipid compositions and detailed structural and functional characterizations by a broad range of surface-sensitive techniques, e.g., neutron reflectometry (NR), quartz crystal microbalance with dissipation monitoring (QCM-D), surface plasmon resonance (SPR), atomic force microscopy (AFM), and fluorescence microscopy.[7,8] At present, most applications of supported lipid

Received: September 10, 2019
Accepted: November 26, 2019
Published: November 26, 2019

DOI: 10.1021/acs.analchem.9b04125
Anal. Chem. XXXX, XXX, XXX−XXX

bilayers focus on studying the interaction between lipid membranes and soluble proteins or peptides. It is an ongoing challenge to produce more complex cell membrane mimics that include different lipid types and correctly oriented membrane proteins.[9]

A few examples are available where membrane proteins were successfully incorporated in lipid bilayers in the proximity of a solid surface.[10−12] The most common strategies are based on either 1) the deposition of proteoliposomes,[11] i.e., protein-loaded liposomes, on solid supports or 2) the chemical anchoring of detergent-reconstituted proteins on the support surface.[13−16] The first approach is not suitable for proteins exhibiting large extramembrane domains and does not allow the protein orientation in the membrane to be controlled. The second approach requires a proper chemical modification of the solid support surface, which often involves gold coating, and a surface functionalization with specific molecular groups for the protein anchoring.[13] A popular strategy is to insert a histidine tag (His-tag) in the primary sequence of the membrane protein such that it can be anchored to the support surface with a defined orientation. Among the advantages of this method are that the membrane protein orientation can indeed be controlled and that a linker can be designed to produce sufficiently large space between the membrane and the support surface to fit large protein extramembrane domains. However, the method involves chemical modifications of both the support surface and the protein sequence, which limits its application to specific surfaces, e.g., using gold-coated supports, and hence specific surface-sensitive techniques and to membrane proteins that can be tagged, e.g., through genetic engineering.

Here, we propose a versatile and efficient method for the preparation of supported lipid bilayers with oriented membrane proteins. The strategy allows membrane proteins with one large extramembrane domain to be oriented in the supported bilayer such that all the reconstituted membrane protein molecules have the large extramembrane domain pointing toward the bulk solvent. It also avoids any sophisticated modification of the support surface or the mandatory introduction of a His-tag in the protein sequence, which minimizes the time and number of steps required for sample preparation.

Supported lipid bilayers with oriented membrane proteins are self-assembled through the unconventional use of a specific kind of nanodiscs, named peptide discs,[17] that we use as carriers of both the lipids and the membrane proteins to the support surface (Figure 1a). Nanodiscs are discoidal lipid bilayers, typically with a diameter around 8−14 nm, that are surrounded and stabilized by two amphipatic belt proteins, the so-called membrane scaffold proteins, MSPs.[18,19] MSP-based nanodiscs have previously been self-assembled to form a film on a solid support surface for the structural investigation of membrane proteins by means of surface-sensitive techniques.[20,21] Although membrane proteins could be successfully oriented in such films, the low surface coverage and the presence of the belt protein within the film were the major limitations of the system.

In contrast to these studies, the present work builds on the application of peptide discs where the nanodisc belt is self-assembled by amphipatic 18A peptide molecules while the interior of the disc still contains a phospholipid bilayer as in the original MSP-based nanodiscs.[17] Such peptide discs have previously been proposed for the reconstitution of membrane proteins,[17,22,23] but they proved less stable over time than classical MSP-based nanodiscs.[17,22] While this instability is clearly a limitation in many applications of the nanodiscs, it is in fact the key property that we exploit in the present work for the assembly of supported lipid membranes. The formation of the peptide disc is a reversible process, which allows the lipids and the membrane proteins to be released on the support surface to form a supported lipid bilayer with incorporated membrane proteins (Figure 1a). We have used the peptide disc deposition on solid supports to produce and characterize supported lipid bilayers with different lipid compositions alone or with two structurally and functionally different membrane proteins, i.e., CorA and tissue factor (TF) (Figure 1b). CorA is a bacterial homopentameric magnesium transporter of known structure.[24,25] The other test system, TF, is a monomeric membrane protein responsible for the initiation of the blood coagulation process.[26] Structural information is so far available only for the TF extracellular domain.[27,28] Besides a few fluorescence resonance energy transfer (FRET) studies,[29,30] there are to the best of our knowledge no experimental data on the structure of the full-length protein in lipid membranes.

In the present study, we tested the method using three different types of solid supports, silicon oxide, mica, and gold, and show that for these surfaces the method works independently of the specific solid support composition and only requires its surface to be hydrophilic. Overall, we found that the nature and quality of the supported bilayers with CorA or TF comply well with the workflow and sample requirements of NR, QCM-D, AFM, and SPR as examples of different surface-sensitive techniques.

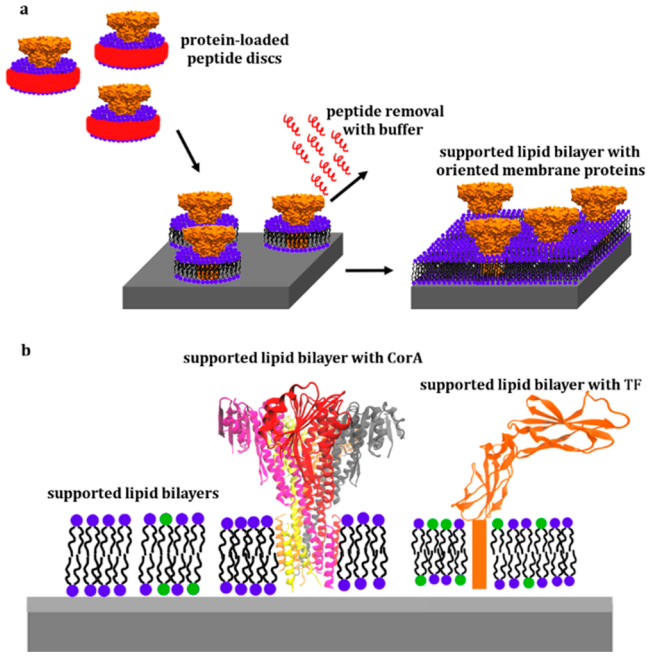

Figure 1. (a) Schematic illustration of the peptide disc mediated formation of a supported lipid bilayer with oriented membrane protein molecules. (b) Schematic representation of the characterized samples. 1-Palmitoyl-2-oleoyl-glycero-3-phosphocholine (POPC) molecules are represented in blue, while 1-palmitoyl-2-oleoyl-*sn*-glycero-3-phospho-L-serine (POPS) molecules are represented in green. The unknown part of the TF structure is illustrated as a rectangle inside the lipid bilayer. [Protein Databank ID: 4EEB, 1DAN].

DOI: 10.1021/acs.analchem.9b04125
Anal. Chem. XXXX, XXX, XXX−XXX

EXPERIMENTAL SECTION

Chemicals. 1-Palmitoyl-2-oleoyl-glycero-3-phosphocholine (POPC) (≥99% purity), 1-palmitoyl-D31-2-oleoyl-*sn*-glycero-3-phosphocholine (dPOPC, ≥ 99% purity), and 1-palmitoyl-2-oleoyl-*sn*-glycero-3-phospho-L-serine (POPS) (≥99% purity) were purchased from Avanti Polar Lipids, Inc. (Alabaster, AL) and used without further purification. 18A peptide (DWLKAFYDKVAEKLKEAF acetylated and amidated at the N-terminal and C-terminal, respectively, >95% purity) was purchased from GenScript and used without further purification. Heavy water (D_2O 99.9% purity), chloroform (≥99.5% purity), ethanol (98% purity), and methanol (99.8% purity) were purchased from Sigma-Aldrich. The activated factor VII (FVIIa) used in this study was provided by NovoNordisk A/S and used without further purification.

Protein Expression and Purification. Professor Mikaela Rapp (University of Stockholm, Sweden) kindly provided the CorA encoding plasmid. Expression and purification was performed as described elsewhere.[31] CorA was stored at −80 °C until use.

Recombinant TF (rTF), containing human TF (1−244) with a linker (G_4S) and a His_6-tag C-terminally was synthesized and cloned into the pET 28a vector by GenScript. A more in-detail protocol is included in a manuscript in preparation. A brief description of the rTF expression and purification is reported in SI-1.

Peptide Disc Preparation and Supported Bilayer Formation. Peptide discs without and with membrane proteins were prepared according to the protocol previously described[17] (see also description in SI-2). For the CorA-loaded peptide discs, a solution of 12 μM CorA (in the buffer of 20 mM Tris−HCl, pH = 7.5, 150 mM NaCl, 0.5 mM EDTA, 0.03% DDM) was added to a POPC (1.3 mM) and 18A (0.43 mM) film and incubated for 1 h. All size exclusion chromatography (SEC) was performed using a Superdex 200 10/300 increase column equilibrated in 20 mM Tris, 100 mM NaCl, 10 mM $CaCl_2$. CorA-loaded peptide discs were readily separated from empty discs using SEC (Figure S1). The collected fractions of CorA-loaded peptide discs were directly used for QCM-D and NR experiments, while a dilution of 1:2 v/v of the sample was applied for AFM measurements. For the rTF-loaded peptide discs with POPC or POPC/POPS (70/30 mol/mol) a solution of 12 μM rTF (in buffer of 20 mM Tris−HCl, pH 7.5, 100 mM NaCl, 0.1% Triton X-100) was added to a POPC (or POPC/POPS) (1.3 mM) and 18A (0.43 mM) film and incubated for 1 h before analyzed using SEC as above (Figure S1). The collected fractions containing a mixture of rTF-loaded and empty discs (see SI-2) were directly used for the QCM-D and SPR analysis. For the NR measurements, the sample was run over a 1 mL HisTrap column (GE Healthcare) equilibrated in 20 mM Tris−HCl, pH 7.5, 100 mM NaCl, 20 mM imidazole and eluted using 20 mM Tris−HCl, pH 7.5, 100 mM NaCl, 250 mM imidazole while collecting fractions of 0.5 mL. This was done to select only TF containing discs. Fractions containing loaded peptide discs were pooled and frozen until use at experiments. The presence of CorA and TF in the peptide discs was confirmed by running the samples on a 15% acrylamide gel (SI-2, Figure S1).

Surface-Sensitive Techniques. Neutron reflectometry experiments were performed on the SURF reflectometer at the ISIS neutron source, Chilton (U.K.). SURF is a horizontal time-of-flight reflectometer. Three incoming angles (θ) typically of 0.35°, 0.65°, and 1.5° were used to cover the q-range of 0.01 Å^{-1} < q < 0.2 Å^{-1}, where $q = \frac{4\pi}{\lambda}\sin(\theta)$. The measured reflected intensity $[I(q)]$ was converted in an absolute reflectivity scale $[R(q)]$ by normalization to the direct beam (I_0) measured at the same slit settings. Slits were chosen to vary with the incident angle in such a way as to provide a constant illumination of the sample (30 mm × 60 mm).

The scattering length density profile $[\rho(z)]$ can be calculated from the experimental reflectivity profiles (eq 1). This gives information on the composition of the sample along the surface normal (z).[32]

$$\rho = \sum_i \frac{n_i b_i}{V_m} \tag{1}$$

where n_i is the number of atoms i, b_i is the coherent scattering length, and V_m is the molecular volume. Further details on NR experimental conditions and data analysis are reported in SI-3. NR measurements were performed in buffer (20 mM Tris−HCl pH = 7.5, 100 mM NaCl, 10 mM $CaCl_2$). The buffer was prepared with different D_2O/H_2O content to achieve three different contrasts with the samples: D_2O buffer (100% D_2O, $\rho = 6.35 \times 10^{-6}$ Å^{-2}), silicon matched water (SMW) buffer (38% D_2O, 62% H_2O, $\rho = 2.07 \times 10^{-6}$ Å^{-2}), and H_2O buffer (100% H_2O, $\rho = -0.56 \times 10^{-6}$ Å^{-2}).

Quartz crystal microbalance with dissipation monitoring was performed with a Q-Sense E4 instrument (Q-Sense, Biolin Scientific AB, Sweden), using SiO_2-coated 5 MHz quartz sensors. Crystals and O-rings were placed in Hellmanex 2% for 10 min, extensively flushed with ethanol and ultrapure water, and then dried under a nitrogen flow. Immediately before use, the crystals were treated with a UV ozone cleaner (BioForce Nanosciences, Inc., Ames, IA) for 20 min. Before acquisition, the fundamental frequency and six overtones (3rd, 5th, 7th, 9th, 11th, and 13th) were recorded and the system was equilibrated in MQ at 25 °C, until stable baselines were obtained. After further equilibration in buffer, the samples were introduced in the flow cell at 0.2 mL/min. During the experiments, real-time shifts in the resonance frequencies (ΔF_n) with respect to the calibration value were measured, with n representing the overtone number. Simultaneously, also the energy dissipation factor (D) was evaluated for all the overtones. The measured ΔF_n is inversely proportional to the adsorbed mass on the sensor.

Atomic force microscopy measurements were carried out using a commercial setup equipped with a liquid cell (MultiMode 8 SPM with a NanoScope V control unit, Bruker AXS). Samples were visualized in 20 mM Tris, 150 mM NaCl buffer pH = 7 at room temperature by operating the AFM in the PeakForce tapping mode. AFM images were acquired at room temperature by using triangular silicon nitride cantilevers with nominal spring constant of 0.7 N m^{-1} and tip radius of 20 nm (ScanAsyst-Fluid, Bruker AXS). Analysis and processing of AFM images was performed with WSxM software.[33] Image processing consisted of plane subtraction/flattening and equalization. Freshly cleaved mica supports were imaged in ultrapure water prior to sample injection to ensure a clean and smooth surface. Then, sample injection and subsequent rinsing with buffer (20 mM Tris, 150 mM NaCl buffer pH = 7.5) was performed in situ as described previously[34] using a slow gravity-fed flow of approximately 50 μL/min.

Surface plasmon resonance measurements were performed with plain unmodified gold sensors (Sensor Chip Au from GE

DOI: 10.1021/acs.analchem.9b04125
Anal. Chem. XXXX, XXX, XXX−XXX

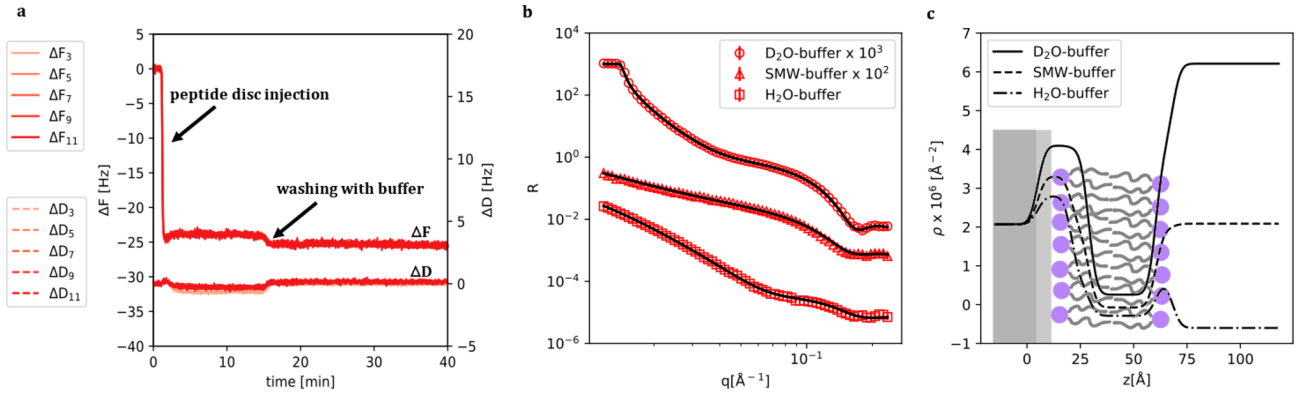

Figure 2. Peptide disc mediated formation of the supported POPC bilayer on SiO_2 surfaces. (a) QCM-D data monitoring the frequency shift ΔF (left y-axis), and the dissipation, ΔD (right y-axis), for the different sensor overtones during formation of the supported POPC bilayer via peptide discs deposition. (b) NR experimental data together with the corresponding fitting curves. Data and fits are rescaled for visualization as indicated in the legend. (c) Scattering length density profiles calculated from experimental data analysis.

Healthcare, cat. no. BR100542) and a Biacore3000 system (GE Healthcare). During the experiments 150 μL of rTF-loaded peptide disc solution in 20 mM Tris, 100 mM NaCl, 20 mM EDTA pH 7.2 was injected at a flow rate of 2 μL/min at 20 °C followed by a stabilization period of 40 min with buffer 20 mM Tris−HCl pH 7.2, 100 mM NaCl, 10 mM $CaCl_2$. The control surface was prepared by injection of the corresponding empty lipid-loaded peptide discs (without rTF). FVIIa binding to rTF embedded in the supported lipid bilayer was probed by injecting 20 nM FVIIa solution at 30 μL/min at 20 °C in 20 mM Tris, 100 mM NaCl, 10 mM $CaCl_2$, pH 7.2 for 250 s followed by 3000 s of dissociation. The sensor chip was regenerated by two consecutive 3 min injections of 20 mM EDTA in running buffer (without Ca^{2+}). This procedure was repeated at different time intervals to probe the stability of the TF-embedded lipid surface. The evaluation software supplied with the instrument for global fitting (Biaevaluation 4.1) was used to calculated the association rate constant (k_{on}) and dissociation rate constant (k_{off}), the K_D (k_{off}/k_{on}), as well as the binding capacity (R_{max}) assuming pseudo-first-order reaction kinetics for a simple bimolecular interaction model.

RESULTS AND DISCUSSION

Peptide Disc Mediated Formation of Supported Lipid Bilayers. Figure 2a shows the QCM-D data collected during the deposition of POPC-loaded peptide discs on a SiO_2-coated quartz sensor. Upon injection of the peptide discs, a rapid decrease in the frequency shift (ΔF) down to ∼−23 Hz with dissipation (ΔD) ∼ 0 was observed suggesting a rapid adsorption of a rigid layer of peptide discs on the support. After about 15 min, the buffer solution was flushed to remove excess peptide discs and to facilitate the removal of the peptide molecules from the deposited lipids. The variation of the ΔF from ∼−23 Hz to ∼−25 Hz together with the variation of ΔD from ∼−0.6 to ∼−0.1 suggests small rearrangements in the deposited film toward the formation of a more compact structure. The ΔF for all of the monitored frequencies reached a stable value of ∼−25 Hz, which is the typical ΔF value observed for the formation of a POPC supported bilayer[35] (see SI-4, Figure S3). NR was applied to obtain more detailed information about the lipid bilayer structure. Parts b and c of Figure 2 show the collected NR data with fitting curves and the corresponding scattering length density profiles, $\rho(z)$, respectively. The model used for data analysis was composed by four layers describing 1) the native silicon oxide layer present on the silicon support surface, 2) the inner lipid headgroup layer, 3) the hydrophobic lipid acyl chains, and 4) the outer lipid headgroup layer (see further details in Figure 2c and SI-3). In the initial analysis, layers 2 and 4 were considered independent. As the bilayer was confirmed to be symmetric, these layers were constrained to have the same parameter values in the final analysis. According to the optimized fitting parameters (SI-5, Table S1), a lipid bilayer was efficiently formed on the support surface (surface coverage >80%) with the expected structural parameters for a POPC membrane.[36] No indications of remaining peptide molecules were detected among the lipid acyl chains.

Similar results were obtained for the supported lipid bilayer prepared using a mixture of POPC and POPS (70/30 mol/mol) in the peptide discs (SI-5, Figure S4). To modify the contrast between the two lipid species, a supported lipid bilayer was also produced by using peptide discs prepared with single-chain deuterated POPC (dPOPC) and POPS (70/30 mol/mol). The contrast between the partially deuterated acyl chains of dPOPC and the hydrogenous chains of POPS allows the POPS concentration in the bilayer to be determined from the ρ value of the bilayer acyl chain region. We found that the POPS content in the supported lipid bilayer produced by the deposition of 18A dPOPC/POPS peptide discs was in perfect agreement with the nominal content of the sample composition, i.e., (28 ± 2)% mol/mol (SI-5 and Table S1). Altogether, the collected data confirms that the peptide discs provide an efficient delivery system to form supported lipid bilayers with relatively high surface coverage and the expected phospholipid composition. The lipid coverage obtained with the peptide discs is comparable to that of vesicle-mediated supported lipid bilayer formation. The deposition of the peptide discs can, however, be conducted in 10−20 s as judged from the QCM-D (Figure 2a). This is much faster than the adsorption and subsequent fusion of the vesicles which typically takes a few minutes (Figure S3). Although only data on POPC and POPC/POPS lipid bilayers are presented here (Figure 2, and SI-S5, Figures S4 and S5) the peptide disc method does not contain any intrinsic limitation to the choice of lipid composition for the lipid bilayer preparation.

Formation of Supported Bilayers with Oriented CorA. Detailed structural information is available for the bacterial magnesium transporter CorA,[24,25] which contains a large

DOI: 10.1021/acs.analchem.9b04125
Anal. Chem. XXXX, XXX, XXX−XXX

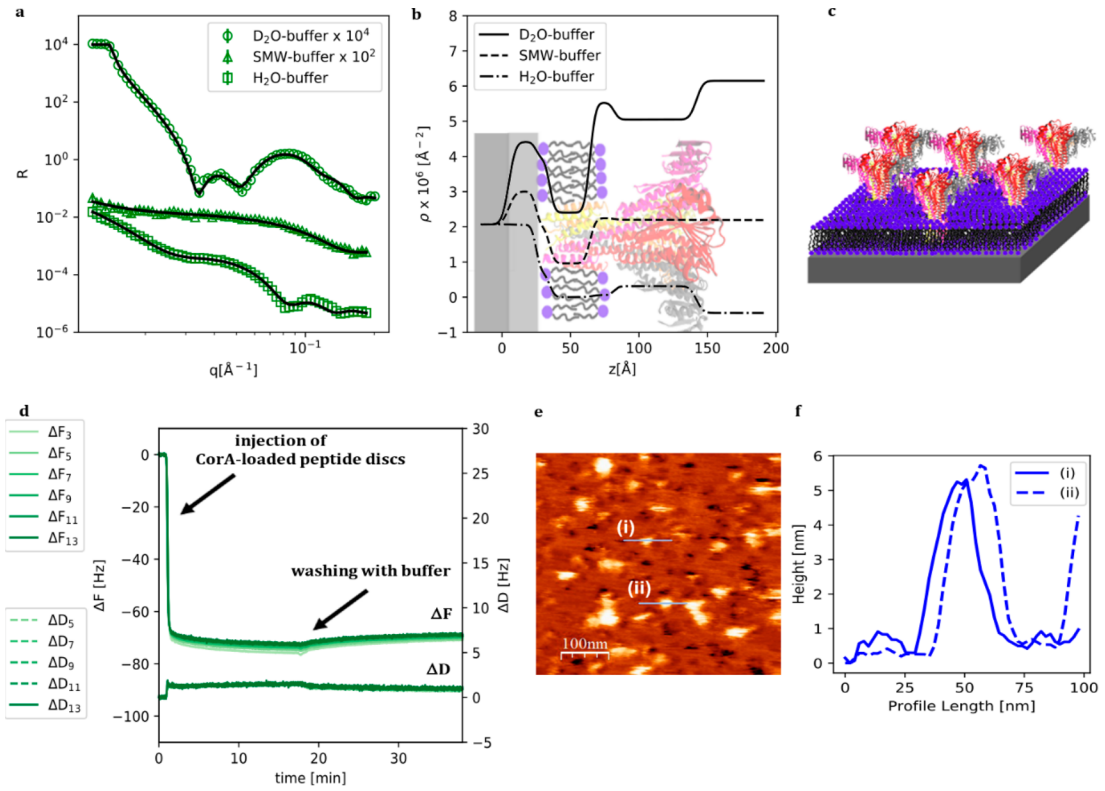

Figure 3. Supported POPC bilayer with CorA. (a) NR experimental data together with the relative fitting curves for the membrane deposited on SiO_2 surface. Data and fits are rescaled for visualization as indicated in the legend. (b) Scattering length density profiles calculated from experimental data analysis. (c) Schematic representation of the supported bilayer with the CorA molecules all sharing the same orientation. (d) QCM-D data monitoring ΔF (left y-axis) and the dissipation ΔD (right y-axis) for the different sensor overtones during the formation of the supported bilayer with CorA on a SiO_2 surface. (e) AFM image collected for the POPC supported bilayer with CorA on mica. In the image the black areas correspond to defects in the supported bilayer. (f) The height profiles corresponding to the blue lines in the AFM image.

extramembrane domain protruding from the intracellular side of the membrane (Figure 1). Furthermore, previous work from our group demonstrated the successful reconstitution of CorA in nanodiscs.[37] In summary, CorA with its large size and good sample control represents an ideal model system to verify that the present method indeed selects a given protein orientation in the deposited lipid bilayer. Parts a and b of Figure 3 show the collected NR experimental data and the derived scattering length density profiles, respectively, for CorA in a supported lipid bilayer. The model for analyzing the NR data was composed by five layers describing 1) silicon oxide layer, 2) inner POPC headgroup layer, which also included CorA extracellular domain (ECD), 3) POPC acyl chain layer and CorA transmembrane domain (TMD), 4) outer POPC headgroup layer, which partially included the CorA intracellular domain (ICD), and 5) the part of the CorA ICD that protrudes out of the membrane surface (see Figure 3 and SI-3). Good model fits to the experimental data were obtained (Figure 3a and SI-6, Table S2) and confirmed the formation of a supported bilayer with all CorA molecules oriented with the large ICD pointing toward the solvent as illustrated in Figure 3c. Alternative orientations of CorA provided very different NR-profiles that were not compatible with the data (see SI-6, Figures S6 and S7). We hypothesize that the favorable interaction between the lipid headgroups and the hydrophilic support surface[38] is the driving force that controls the membrane protein orientation. Only if the large ICD is oriented away from the support the lipid headgroups become sufficiently close and can stably interact with the support surface. Our analysis shows that a large volume fraction of the CorA ICD (35% v/v) and TMD (20% v/v) was obtained in the prepared supported bilayers. Although the overall membrane surface coverage was 64% v/v, according to the 36% v/v of solvent in the layer containing the lipid acyl chains and the CorA−TMD (SI-6, Table S2), the collected data still represents one of very few examples of high protein loading in supported lipid bilayers.[15]

Peptide disc formed supported bilayers with CorA were also investigated by means of complementary surface-sensitive techniques such as QCM-D and AFM to evaluate compatibility with these methods. As for the peptide discs prepared with lipids only, the deposition of CorA-loaded peptide discs on the quartz sensor is a fast process that, in a few minutes, leads to a stable ΔF signal (Figure 3d) of a clearly more pronounced magnitude than the one corresponding to the pure lipid bilayer (Figure 2a). Buffer flushing through the cell produced a small increase of ΔF, which reached a stable value close to −69 Hz. Altogether, the recorded ΔF values are consistent with the formation of a supported bilayer with a high protein content.

Figure 3e shows an AFM image collected for the POPC supported bilayer with CorA on a mica substrate. The AFM image clearly shows the presence of features protruding out of the membrane plane. Most of these features exhibited a width at half-height of approximately 20 nm and heights in the 4−7 nm range (Figure 3f), similar to those determined from the NR data analysis for the CorA ICD thickness (SI-6, Table S2). The higher width values can be attributed to tip dilation effects,[39] i.e., imaging of features smaller than the AFM tip results in

DOI: 10.1021/acs.analchem.9b04125
Anal. Chem. XXXX, XXX, XXX−XXX

width values similar to those of the tip (approximately 20 nm). Thus, it is reasonable to attribute the smaller visualized features to CorA, although the resolution does not allow us to verify whether CorA is in its native pentameric state. The total area of the features associated with CorA in Figure 3e is approximately 15% of the image total area (tip dilation might affect this result since CorA-ICD is much smaller than the AFM tip). By taking into account the dilution of the sample used for AFM compared to the one used for the NR measurements, the CorA ICD coverage estimated by AFM is overall in good agreement with the value obtained from NR data analysis. Larger features were also present in the sample. Higher resolution AFM images (SI-7, Figure S8) revealed that these larger features also consisted of CorA and indicated a tendency for self-association beyond the native pentameric state, which might occur through lateral diffusion of CorA in the supported bilayer.

Formation of Supported Bilayers with Tissue Factor. A modified version of TF, named recombinant TF, rTF, was used in this study (see the Experimental Section). While the rTF ECD and TMD are the same as in the native TF, the composition of the ICD is different in the two proteins. This modification of the protein sequence is required for an efficient protein purification. Although rTF ICD (~12 residues) and TF ICD (~19 residues) have different amino acid composition, they still exhibit an overall similar size, which makes rTF a suitable candidate to mimic TF. Figure 4 shows

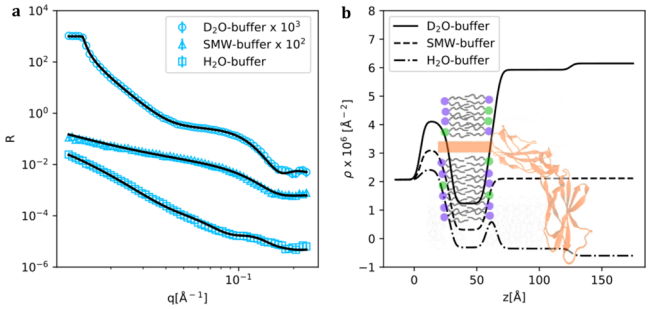

Figure 4. (a) NR experimental data together with the relative fitting curves for the supported bilayer with rTF and lipid composition POPC/POPS (70/30 mol/mol). Data and fits are rescaled for visualization as indicated in the legend. (b) Scattering length density profile calculated from experimental data analysis.

the NR data collected for the POPC/POPS (70/30 mol/mol) supported bilayer with rTF. Data modeling was based on the same schematic representation of the membrane protein used in the case of CorA. However, in rTF, the ICD is a very short domain while the ECD is a larger domain (~219 residues). The consistency between the experimental data and fitting curves confirmed the orientation of rTF in the lipid membrane with the ECD exposed to the solvent (SI-S8, Figures S9 and S10).

rTF is considerably smaller than CorA and is expected to have a smaller volume fraction in the prepared lipid bilayer. Conversion to mole fraction shows that the protein contents in the supported bilayers with CorA and rTF are actually quite similar ~0.6% mol/mol (protein−TMD/lipids) for rTF and ~0.4% mol/mol (protein−TMD/lipids) for CorA. In this calculation pentameric CorA is assumed in the lipid bilayer. The NR data also provided the thickness associated with the rTF ECD protruding out of the bilayer surface as 59 ± 5 Å, which notably is considerably shorter than the maximum length of the protein domain (i.e., 75 Å[28]). This suggests that the rTF ECD is on average tilted toward the lipid headgroups as sketched in Figure 4. The activated coagulation factor VII (FVIIa) is a soluble protein and the native binding partner for rTF. Hence, demonstrating a robust binding of FVIIa to rTF ECD in the produced supported bilayers with the expected kinetic rate constants is a fundamental acid test of the mimicry that is achieved by this surrogate lipid bilayer. QCM-D and SPR were used to monitor the binding of FVIIa to the supported bilayer with rTF. As FVIIa is reported to interact with phosphatidylserine (PS) lipids independent of TF,[27] these experiments were performed using a POPC supported bilayer, which indeed exhibited very little affinity for FVIIa in the absence of rTF (SI-9, Figures S11 and S12). Parts a and b of Figure 5 show the initial formation of the supported POPC bilayer with rTF. Addition of FVIIa produced a large ΔF decrease, consistent with an increase of the adsorbed mass on the sensor surface. Since FVIIa does not stably adsorb on a pure POPC bilayer, the observed ΔF decrease signifies FVIIa binding to rTF. This result qualitatively confirms that the rTF-ECD was in a binding-competent stage. Figure 5c shows the difference in SPR signals during the deposition of a POPC supported bilayer in the reference flow cell (red curve) and the supported bilayer with rTF in the active flow cell (blue curve). The difference in the immobilized mass between the reference (supported POPC bilayer) and the active surface (supported POPC bilayer with TF) was estimated to be 100−200 RU after 6000 s suggesting that 3.5−7 fmols of TF/mm^2 was deposited in the active flow cell. This corresponds to a surface coverage of around 2−4% of the TF ECD. Injection of FVIIa over the bilayer revealed a specific binding of FVIIa to the surface with embedded rTF yielding an equilibrium dissociation constant K_D of 0.2 × 10^{-9} M (Figure 5c, SI-9, Table S4), in agreement with previously reported results.[40]

CONCLUSION

The use of phospholipid and membrane protein loaded peptide discs represents a versatile approach for the production of supported lipid bilayers with membrane proteins, which offers several unique advantages compared to other state-of-the-art methods. In particular, no chemical modification of the support is required. Solid supports with different chemical compositions can be successfully used, as long as the surface is hydrophilic. Also, no binding tag of the membrane protein is needed to control the protein orientation. Since the membrane proteins are not chemically anchored to the support, they are, in principle, free to diffuse laterally within the bilayer, as they are in native cell membranes. Two different kinds of membrane proteins, CorA and TF, were efficiently loaded in the peptide discs and used to validate the proposed method for the formation of supported lipid bilayers with membrane proteins. CorA was used as a model system to validate the production of a supported lipid bilayer with a high concentration of oriented CorA as determined by NR. The peptide disc mediated deposition of rTF allowed us to produce a relevant model system for TF in a native-like lipid environment. NR analysis of the produced rTF containing bilayers confirmed a structure with oriented rTF and the extracellular domain pointing toward the bulk solvent. The samples were used to probe the interaction between rTF and its soluble binding partner FVIIa by QCM-D and SPR and demonstrated that the incorporated rTF was indeed binding-competent.

DOI: 10.1021/acs.analchem.9b04125
Anal. Chem. XXXX, XXX, XXX−XXX

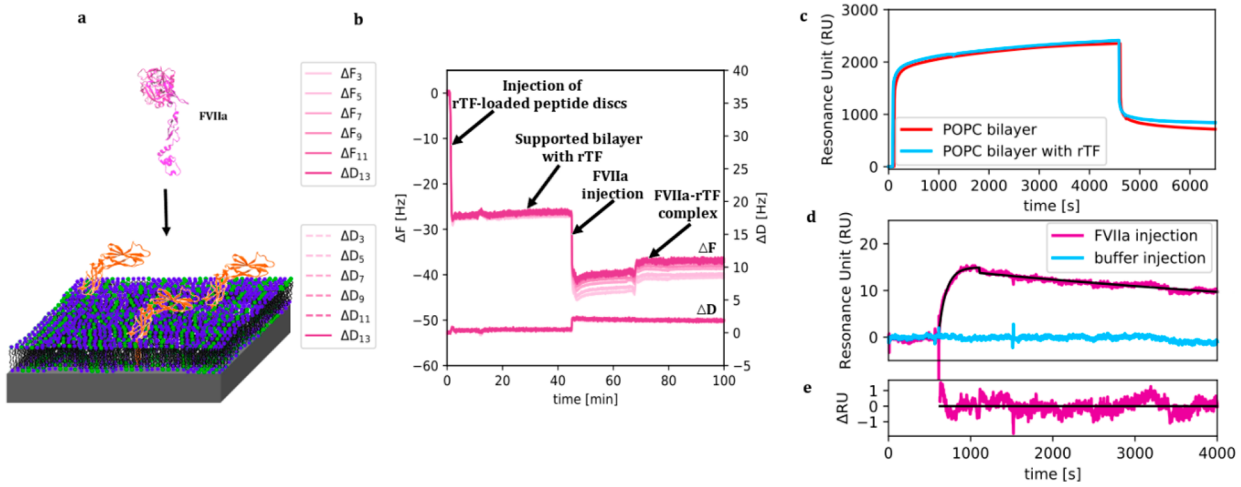

Figure 5. (a) Schematic representation of the interaction between FVIIa and the supported bilayer with rTF. (b) QCM-D data for the supported POPC bilayer with rTF on a SiO_2 surface; the frequency shift, ΔF (left *y*-axis), and the dissipation, ΔD (right *y*-axis), for the different sensor overtones are monitored over time. (c) Comparison between the SPR data collected during the formation of the supported POPC bilayer with (blue curve, active flow cell) and without rTF (red curve, reference flow cell) on a Au surface. (d) Real-time binding of FVIIa (20 nM) to the supported POPC bilayer with rTF (magenta curve, active flow cell) with double-reference subtraction, i.e., the signal from a POPC supported lipid during FVIIa injection was first subtracted followed by the signal from a buffer injection (blue curve). The blue curve shows a buffer injection demonstrating the stability of the supported bilayer with rTF. The fit to a simple bimolecular interaction model is reported in black. (e) Residual (ΔRU) plot for the fit in panel d.

Both lipid−substrate and protein−substrate interaction can play crucial role in defining the in-plane orientation of membrane proteins. However, based on the current study and a previous report,[41] a certain degree of in-plane asymmetry in the protein structure appears to be an important factor for orienting the membrane protein molecules on the support surface. Future experiments will be dedicated to extend the method to additional membrane proteins with different structure.

■ ASSOCIATED CONTENT

Supporting Information

The Supporting Information is available free of charge at https://pubs.acs.org/doi/10.1021/acs.analchem.9b04125.

Supplementary description of sample preparation and NR data analysis, additional QCM-D and NR data on supported lipid bilayers, and additional AFM image of the supported lipid bilayer with CorA (PDF)

■ AUTHOR INFORMATION

Corresponding Authors

*E-mail: a.luchini@nbi.ku.dk.
*E-mail: arleth@nbi.ku.dk.

ORCID

Alessandra Luchini: 0000-0003-2380-6069
Nicolai Tidemand Johansen: 0000-0002-8596-548X
Marité Cárdenas: 0000-0003-0392-3540
Lise Arleth: 0000-0001-6694-0626

Notes

The authors declare no competing financial interest.

■ ACKNOWLEDGMENTS

The work was supported by the Novo Nordisk Foundation "SYNERGY", the Lundbeck Foundation "BRAINSTRUC" project, and Danish Research Council Danscatt program. The authors thank the ISIS neutron source for beamtime allocation (https://doi.org/10.5286/ISIS.E.RB1820625 and https://doi.org/10.5286/ISIS.E.RB1910248).

■ REFERENCES

(1) Rawlings, A. E. *Biochem. Soc. Trans.* **2016**, *44* (3), 790−5.
(2) Lyu, S. W.; Wang, J. F.; Chao, L. *Sci. Rep.* **2019**, *9* (1), 2747.
(3) van Weerd, J.; Karperien, M.; Jonkheijm, P. *Adv. Healthcare Mater.* **2015**, *4* (18), 2743−2779.
(4) Andersson, J.; Koper, I.; Knoll, W. *Front. Mater.* **2018**, *5*, 55.
(5) Isaksson, S.; Watkins, E. B.; Browning, K. L.; Kjellerup Lind, T.; Cárdenas, M.; Hedfalk, K.; Höök, F.; Andersson, M. *Nano Lett.* **2017**, *17* (1), 476−485.
(6) Jagalski, V.; Barker, R. D.; Thygesen, M. B.; Gotfryd, K.; Krüger, M. B.; Shi, L.; Maric, S.; Bovet, N.; Moulin, M.; Haertlein, M.; Günther Pomorski, T.; Loland, C. J.; Cárdenas, M. *Soft Matter* **2015**, *11* (39), 7707−7711.
(7) Pace, H. P.; Hannestad, J. K.; Armonious, A.; Adamo, M.; Agnarsson, B.; Gunnarsson, A.; Micciulla, S.; Sjövall, P.; Gerelli, Y.; Höök, F. *Anal. Chem.* **2018**, *90* (21), 13065−13072.
(8) Kiessling, V.; Yang, S.-T.; Tamm, L. K. Supported Lipid Bilayers as Models for Studying Membrane Domains. In *Current Topics in Membranes*; Kenworthy, A. K., Ed.; Academic Press: Waltham, MA, 2015; Vol. *75*, pp 1−23.
(9) Fragneto, G.; Delhom, R.; Joly, L.; Scoppola, E. *Curr. Opin. Colloid Interface Sci.* **2018**, *38*, 108−121.
(10) Pace, H.; Simonsson Nyström, L. S.; Gunnarsson, A.; Eck, E.; Monson, C.; Geschwindner, S.; Snijder, A.; Hook, F. *Anal. Chem.* **2015**, *87* (18), 9194−9203.
(11) Graneli, A.; Rydstrom, J.; Kasemo, B.; Hook, F. *Langmuir* **2003**, *19* (3), 842−850.
(12) Heinrich, F.; Losche, M. *Biochim. Biophys. Acta, Biomembr.* **2014**, *1838* (9), 2341−9.
(13) Giess, F.; Friedrich, M. G.; Heberle, J.; Naumann, R. L.; Knoll, W. *Biophys. J.* **2004**, *87* (5), 3213−3220.
(14) Le Brun, A. P.; Haigh, C. L.; Drew, S. C.; James, M.; Boland, M. P.; Collins, S. J. *Biophys. J.* **2014**, *107* (10), 2313−2324.
(15) McGillivray, D. J.; Valincius, G.; Heinrich, F.; Robertson, J. W. F.; Vanderah, D. J.; Febo-Ayala, W.; Ignatjev, I.; Lösche, M.; Kasianowicz, J. J. *Biophys. J.* **2009**, *96* (4), 1547−1553.

DOI: 10.1021/acs.analchem.9b04125
Anal. Chem. XXXX, XXX, XXX−XXX

(16) Holt, S. A.; Le Brun, A. P.; Majkrzak, C. F.; McGillivray, D. J.; Heinrich, F.; Losche, M.; Lakey, J. H. *Soft Matter* **2009**, *5* (13), 2576−2586.
(17) Midtgaard, S. R.; Pedersen, M. C.; Kirkensgaard, J. J. K.; Sørensen, K. K.; Mortensen, K.; Jensen, K. J.; Arleth, L. *Soft Matter* **2014**, *10* (5), 738−752.
(18) Bayburt, T. H.; Sligar, S. G. *FEBS Lett.* **2010**, *584* (9), 1721−1727.
(19) Skar-Gislinge, N.; Kynde, S. A. R.; Denisov, I. G.; Ye, X.; Lenov, I.; Sligar, S. G.; Arleth, L. *Acta Crystallogr., Sect. D: Biol. Crystallogr.* **2015**, *71* (12), 2412−2421.
(20) Bertram, N.; Laursen, T.; Barker, R.; Bavishi, K.; Møller, B. L.; Cardenas, M. *Langmuir* **2015**, *31* (30), 8386−8391.
(21) Wadsater, M.; Laursen, T.; Singha, A.; Hatzakis, N. S.; Stamou, D.; Barker, R.; Mortensen, K.; Feidenhans'l, R.; Møller, B. L.; Cardenas, M. *J. Biol. Chem.* **2012**, *287* (41), 34596−34603.
(22) Larsen, A. N.; Sorensen, K. K.; Johansen, N. T.; Martel, A.; Kirkensgaard, J. J.; Jensen, K. J.; Arleth, L.; Midtgaard, S. R. *Soft Matter* **2016**, *12* (27), 5937−49.
(23) Carlson, M. L.; Young, J. W.; Zhao, Z.; Fabre, L.; Jun, D.; Li, J.; Li, J.; Dhupar, H. S.; Wason, I.; Mills, A. T.; Beatty, J. T.; Klassen, J. S.; Rouiller, I.; Duong, F. *eLife* **2018**, *7*, e34085.
(24) Lunin, V. V.; Dobrovetsky, E.; Khutoreskaya, G.; Zhang, R.; Joachimiak, A.; Doyle, D. A.; Bochkarev, A.; Maguire, M. E.; Edwards, A. M.; Koth, C. M. *Nature* **2006**, *440* (7085), 833−837.
(25) Matthies, D.; Dalmas, O.; Borgnia, M. J.; Dominik, P. K.; Merk, A.; Rao, P.; Reddy, B. G.; Islam, S.; Bartesaghi, A.; Perozo, E.; Subramaniam, S. *Cell* **2016**, *164* (4), 747−756.
(26) Mackman, N. *J. Thromb. Haemostasis* **2009**, *7*, 136−9.
(27) Ansari, S. A.; Pendurthi, U. R.; Sen, P.; Rao, L. V. M. *PLoS One* **2016**, *11* (6), e0158377.
(28) Banner, D. W.; D'Arcy, A.; Chene, C.; Winkler, F. K.; Guha, A.; Konigsberg, W. H.; Nemerson, Y.; Kirchhofer, D. *Nature* **1996**, *380* (6569), 41−46.
(29) McCallum, C. D.; Hapak, R. C.; Neuenschwander, P. F.; Morrissey, J. H.; Johnson, A. E. *J. Biol. Chem.* **1996**, *271* (45), 28168−75.
(30) McCallum, C. D.; Su, B.; Neuenschwander, P. F.; Morrissey, J. H.; Johnson, A. E. *J. Biol. Chem.* **1997**, *272* (48), 30160−6.
(31) Palombo, I.; Daley, D. O.; Rapp, M. *J. Biol. Chem.* **2012**, *287* (33), 27547−27555.
(32) Fragneto-Cusani, G. *J. Phys.: Condens. Matter* **2001**, *13* (21), 4973−4989.
(33) Horcas, I.; Fernandez, R.; Gomez-Rodriguez, J. M.; Colchero, J.; Gomez-Herrero, J.; Baro, A. M. *Rev. Sci. Instrum.* **2007**, *78* (1), 013705.
(34) Lind, T. K.; Cardenas, M. *Biointerphases* **2016**, *11* (2), 020801.
(35) Lind, T. K.; Cardenas, M.; Wacklin, H. P. *Langmuir* **2014**, *30* (25), 7259−7263.
(36) Luchini, A.; Nzulumike, A. N. O.; Lind, T. K.; Nylander, T.; Barker, R.; Arleth, L.; Mortensen, K.; Cárdenas, M. *Colloids Surf., B* **2019**, *173*, 202−209.
(37) Johansen, N. T.; Pedersen, M. C.; Porcar, L.; Martel, A.; Arleth, L. *Acta Crystallographica Section D* **2018**, *74* (12), 1178−1191.
(38) Anderson, T. H.; Min, Y.; Weirich, K. L.; Zeng, H.; Fygenson, D.; Israelachvili, J. N. *Langmuir* **2009**, *25* (12), 6997−7005.
(39) Margeat, E.; Le Grimellec, C.; Royer, C. A. *Biophys. J.* **1998**, *75* (6), 2712−20.
(40) Sen, P.; Neuenschwander, P. F.; Pendurthi, U. R.; Rao, L. V. *Blood Coagulation Fibrinolysis* **2010**, *21* (4), 376−9.
(41) Bao, P.; Cartron, M. L.; Sheikh, K. H.; Johnson, B. R. G.; Hunter, C. N.; Evans, S. D. *Chem. Commun.* **2017**, *53* (30), 4250−4253.

NOTE ADDED AFTER ASAP PUBLICATION

After this paper was published on December 10, 2019, a correction was made to Figure 4 (SMW-buffer and H_2O-buffer plots were reversed). The corrected version was reposted December 11, 2019.

DOI: 10.1021/acs.analchem.9b04125
Anal. Chem. XXXX, XXX, XXX−XXX